Journal of Nanophotonics

SPIEDigitalLibrary.org/jnp

Excitation of multiple surface-plasmon-polariton waves using a compound surface-relief grating

Muhammad Faryad
Akhlesh Lakhtakia

SPIE

Excitation of multiple surface-plasmon-polariton waves using a compound surface-relief grating

Muhammad Faryad and Akhlesh Lakhtakia
Pennsylvania State University, Department of Engineering Science and Mechanics, Nanoengineered Metamaterials Group (NanoMM), University Park, Pennsylvania 16802-6812
akhlesh@psu.edu

Abstract. The excitation of multiple surface-plasmon-polariton waves, all of the same frequency but different polarization states, phase speeds, spatial profiles and degrees of localization, by a compound surface-relief grating formed by a metal and a rugate filter, both of finite thickness, was studied using the rigorous coupled-wave approach. Each period of the compound surface-relief grating was chosen to have an integral number of periods of two different simple surface-relief gratings. The excitation of different SPP waves was inferred from the absorptance peaks that were independent of the thickness of the rugate filter. The excitation of each SPP wave could be attributed to either a simple surface-relief grating present in the compound surface-relief grating or to the compound surface-relief grating itself. However, the excitation of SPP waves was found to be less efficient with the compound surface-relief grating than with a simple surface-relief grating. © *2012 Society of Photo-Optical Instrumentation Engineers (SPIE).* [DOI: 10.1117/1.JNP.6.061701]

Keywords: grating coupling; rugate filter; surface multiplasmonics.

Paper 12064SS received Jun. 9, 2012; revised manuscript received Jul. 11, 2012; accepted for publication Jul. 11, 2012; published online Oct. 5, 2012.

1 Introduction

The solution of a canonical boundary-value problem demonstrates that the planar interface of (1) a semi-infinite metal, and (2) a semi-infinite homogeneous, isotropic, dielectric material can guide one surface plasmon-polariton (SPP) wave, at a specific frequency and in a specific direction lying in the interface plane.[1,2] This SPP wave is of the *p*-polarization state. In practice, SPP waves are excited in the prism-coupled and the grating-coupled configurations. The prism-coupled configuration is widely used for chemical sensing.[2] Whereas the grating-coupled configuration has been known for at least three decades to be useful in enhancing the absorptance of solar cells,[3,4] this enhancement has only recently been interpreted in terms of SPP waves.[5,6]

In the grating-coupled configuration, the planar interface is replaced by one with periodic corrugations. This interface is a surface-relief grating. Light is then incident on the other face of the partnering dielectric material. The electromagnetic field phasors are expressed in terms of Floquet harmonics. If the period of the surface-relief grating is appropriate, a part of the incident light may couple to the SPP wave at a certain value of the incidence angle. This happens when one of the Floquet harmonics has a wavevector with a component parallel to the mean plane of the grating the same as the real part of the possible SPP wave.[2,7]

Recently, to enhance the possibility of this match occurring, Dolev et al.[8] made the surface-relief grating a compound grating, called a quasiperiodic grating by them. Each period of the compound grating comprises several periods each of more than one simple surface-relief gratings. Dolev et al.[8] showed that such a compound grating can be advantageously used to excite the same *p*-polarized SPP wave at different angles of incidence.

Multiple SPP waves of the same frequency and direction of propagation, but with different phase speeds, spatial profiles, and degrees of localizations, can be guided by the planar interface of a metal and a dielectric material that is periodically nonhomogeneous normal to the interface, whether that interface is either planar[9] or a simple surface-relief grating.[10] The multiplicity offers

0091-3286/2012/$25.00 © 2012 SPIE

exciting prospects for enhancing the scope of applications of SPP waves.[11,12] Chief among these are multianalyte chemical sensors[13] and thin-film solar cells.[14] The higher the number of SPP waves that can be excited, the more attractive are the prospects.

Although multiple SPP waves can be excited in the grating-coupled configuration,[10] in line with predictions from the solution of the canonical boundary-value problem,[9] a simple surface-relief grating may not suffice for the excitation of all possible SPP waves. With simple surface-relief gratings of different periods, different subsets of the possible SPP waves may be excited,[10] which limits the benefits resulting from multiple SPP waves. Therefore, we decided to investigate whether a compound surface-relief grating would be better than a simple surface-relief grating.

Let us note the important difference between the work presented here and that of Dolev et al.:[8] the partnering dielectric material in our work is periodically nonhomogeneous normal to the mean metal/dielectric interface, allowing the excitation of multiple SPP waves of the same frequency but different linear polarization states, phase speeds, and spatial profiles, thereby in contrast to Dolev et al.[8] whose partnering dielectric material is homogeneous.

Because the theoretical formulation of the boundary-value problem discussed in this paper is the same as in Ref. 10, only a brief overview of the formulation is provided in Sec. 2. Illustrative numerical results are presented and discussed in Sec. 3, and the concluding remarks are presented in Sec. 4. An $\exp(-i\omega t)$ time-dependence is implicit, with ω denoting the angular frequency. The free-space wavenumber, the free-space wavelength, and the intrinsic impedance of free space are denoted by $k_0 = \omega\sqrt{\epsilon_0\mu_0}$, $\lambda_0 = 2\pi/k_0$, and $\eta_0 = \sqrt{\mu_0/\epsilon_0}$, respectively, with μ_0 and ϵ_0 being the permeability and permittivity of free space. Vectors are in boldface, the asterisk denotes the complex conjugate, and the Cartesian unit vectors are identified as $\hat{\mathbf{u}}_x$, $\hat{\mathbf{u}}_y$, and $\hat{\mathbf{u}}_z$. The real part of a complex number ζ is denoted by $\mathrm{Re}(\zeta)$.

2 Boundary-Value Problem

Let us consider the boundary-value problem shown schematically in Fig. 1. The regions $z < 0$ and $z > d_3$ are vacuous. The region $0 \le z \le d_1$ is occupied by a rugate filter[15,16] with relative permittivity

$$\epsilon_d(z) = \left[\left(\frac{n_b + n_a}{2}\right) + \left(\frac{n_b - n_a}{2}\right)\sin\left(\pi\frac{d_2 - z}{\Omega}\right)\right]^2, \qquad z > 0, \tag{1}$$

where 2Ω is the period, and n_a and n_b are the lowest and the highest indexes of refraction, respectively. Such filters can be deposited on top of a metallic film with a corrugated surface

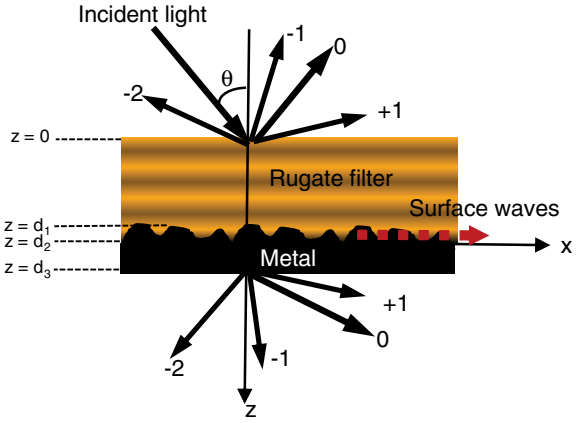

Fig. 1 Schematic of the grating-coupled configuration used for the excitation of multiple SPP waves by an incident plane wave. Specular reflection and transmission are denoted by order $n = 0$, whereas nonspecular modes are denoted by orders $n \neq 0$. The SPP waves are guided by the periodically corrugated metal/rugate-filter interface.

with a variety of well-established techniques.[17–19] The region $d_2 \le z \le d_3$ is occupied by the metallic partnering material with spatially uniform relative permittivity ϵ_m.

The region $d_1 < z < d_2$ contains a compound surface-relief grating of period L along the x axis. The relative permittivity $\epsilon_g(x,z) = \epsilon_g(x \pm L, z)$ in this region is taken to be as

$$\epsilon_g(x,z) = \epsilon_m - [\epsilon_m - \epsilon_d(z)]\mathcal{U}[d_2 - z - g(x)], \qquad x \in (0, L), \tag{2}$$

for $z \in (d_1, d_2)$, with

$$g(x) = \begin{cases} \frac{1}{2}(d_2 - d_1)\left[1 + \sin\left(2\pi \frac{x}{\Lambda_1}\right)\right], & x \in (0, L_1), \\ \frac{1}{2}(d_2 - d_1)\left[1 + \sin\left(2\pi \frac{x - L_1}{\Lambda_2}\right)\right], & x \in (L_1, L), \end{cases} \tag{3}$$

and

$$\mathcal{U}(\zeta) = \begin{cases} 1, & \zeta \ge 0, \\ 0, & \zeta < 0. \end{cases} \tag{4}$$

The chosen compound surface-relief grating is made of two simple surface-relief gratings, one of period Λ_1 and the other of period Λ_2. Both of the simple gratings have a sinusoidal profile. For simplicity, both simple gratings have the same crest-to-trough distance $d_2 - d_1$, and the depth L_g of the compound surface-relief grating therefore is also the same: $L_g = d_2 - d_1$. Each period of the compound grating comprises N_1 consecutive periods of the simple grating with period Λ_1 and N_2 consecutive periods of the simple grating with period Λ_2; hence, $L = L_1 + L_2$, $L_1 = N_1\Lambda_1$ ($N_1 \in \{1, 2, 3, \ldots\}$), and $L_2 = N_2\Lambda_2$ ($N_2 \in \{1, 2, 3, \ldots\}$).

We chose this particular grating-shape function $g(x)$ because sinusoidal surface-relief gratings are the easiest type of grating for theoretical studies of the excitation of SPP waves.[7] Simple gratings with nonsinusoidal profiles can be investigated with the theoretical formulation adopted here.[10] Furthermore, more than two simple gratings can be incorporated in a compound grating.

In the vacuous half-space $z \le 0$, let a plane wave propagating in the xz plane at an angle θ to the z axis, be incident on the compound surface-relief grating coated with the rugate filter. Hence, the incident, reflected, and transmitted electric field phasors may be written in terms of Floquet harmonics as follows:

$$\mathbf{E}_{\rm inc}(r) = \sum_{n=-N_t}^{n=N_t} (\mathbf{s}_n a_s^{(n)} + \mathbf{p}_n^+ a_p^{(n)}) \exp[i(k_x^{(n)} x + k_z^{(n)} z)], \qquad z \le 0, \tag{5}$$

$$\mathbf{E}_{\rm ref}(r) = \sum_{n=-N_t}^{n=N_t} (\mathbf{s}_n r_s^{(n)} + \mathbf{p}_n^- r_p^{(n)}) \exp[i(k_x^{(n)} x - k_z^{(n)} z)], \qquad z \le 0, \tag{6}$$

$$\mathbf{E}_{\rm tr}(r) = \sum_{n=-N_t}^{n=N_t} (\mathbf{s}_n t_s^{(n)} + \mathbf{p}_n^+ t_p^{(n)}) \exp\{i[k_x^{(n)} x + k_z^{(n)}(z - d_3)]\}, \qquad z \ge d_3. \tag{7}$$

Here,

$$k_x^{(n)} = k_0 \sin\theta + n\kappa_x \tag{8}$$

is the wavenumber of the Floquet harmonic of order n, with

$$\kappa_x = \frac{2\pi}{L} = \frac{2\pi}{N_1 L_1 + N_2 L_2}, \tag{9}$$

and

$$k_z^{(n)} = \begin{cases} +\sqrt{k_0^2 - (k_x^{(n)})^2}, & k_0^2 > (k_x^{(n)})^2 \\ +i\sqrt{(k_x^{(n)})^2 - k_0^2}, & k_0^2 < (k_x^{(n)})^2 \end{cases}. \tag{10}$$

The s and p-polarization states are represented, respectively, by

$$\mathbf{s}_n = \hat{\mathbf{u}}_y \tag{11}$$

and

$$\mathbf{p}_n^{\pm} = \mp \frac{k_z^{(n)}}{k_0}\hat{\mathbf{u}}_x + \frac{k_x^{(n)}}{k_0}\hat{\mathbf{u}}_z. \tag{12}$$

The coefficients $a_s^{(n)} = a_p^{(n)} = 0 \quad \forall\, n \in [-N_t, N_t]$, except that $a_s^{(0)} \neq 0$ when the incident plane wave is s-polarized and $a_p^{(0)} \neq 0$ when the incident plane wave is p-polarized. The coefficients $r_{s,p}^{(n)}$ and $t_{s,p}^{(n)}$ have to be determined by solving a boundary-value problem.

That boundary-value problem was formulated using the rigorous coupled-wave approach (RCWA)[20,21] and was implemented using a stable algorithm.[22–24] The accuracy of the solution using RCWA depends on the value of N_t, the number of terms of Floquet harmonics in the representation of field phasors being $2N_t + 1$. The formulation of the boundary-value problem and the numerical algorithm have been explained elsewhere in detail[10] and we skip both to go directly to present representative numerical results in Sec. 3.

3 Numerical Results and Discussion

For illustrative numerical results, we chose a rugate filter with $\Omega = \lambda_0$, $n_a = 1.45$ and $n_b = 2.32$ (Ref. 10). We set the free-space wavelength $\lambda_0 = 633$ nm and chose the metal to be bulk aluminum ($\epsilon_{\text{met}} = -56 + 21i$).

The plane wave absorptance of the entire structure depicted in Fig. 1 is given by

$$A = 1 - \sum_{n=-N_t}^{N_t} \frac{|r_s^{(n)}|^2 + |r_p^{(n)}|^2 + |t_s^{(n)}|^2 + |t_p^{(n)}|^2}{|a_s^{(0)}|^2 + |a_p^{(0)}|^2} \text{Re}\left(\frac{k_z^{(n)}}{k_z^{(0)}}\right). \tag{13}$$

The absorptance for p-polarized incidence is denoted by $A_p = A|_{a_s^{(0)}=0, a_p^{(0)}\neq 0}$, and that for s-polarized incidence by $A_s = A|_{a_s^{(0)}\neq 0, a_p^{(0)}=0}$. Let us note that $r_s^{(n)} = 0$ and $t_s^{(n)} = 0 \;\forall\, n \in [-N_t, N_t]$ for p-polarized incident plane waves, and vice versa for the s-polarized case, because the partnering dielectric material is isotropic.

We implemented the RCWA in Mathematica and calculated the absorptances A_p and A_s as functions of θ. We fixed $N_t = 40$ after ascertaining that the absorptances for $N_t = 40$ converged to within $\pm 1\%$ of the absorptances calculated with $N_t = 41$. Also, the electric field phasor $\mathbf{E}(x, z)$, the magnetic field phasor $\mathbf{H}(x, z)$, and the time-averaged Poynting vector

$$\mathbf{P}(x, z) = \frac{1}{2}\text{Re}[\mathbf{E}(x, z) \times \mathbf{H}^*(x, z)], \tag{14}$$

were calculated as appropriate. For this purpose, the region $0 < z < d_1$ was divided into 3-nm-thick slices parallel to the plane $z = 0$, the grating region ($d_1 < z < d_2$) was divided into 1-nm-thick slices, but the metallic layer ($d_2 < z < d_3$) was kept as one slice.

3.1 *Canonical Boundary-Value Problem*

The corresponding canonical boundary-value problem, when both the rugate filter and the metal are semi-infinite in thickness and their interface is planar, has been solved elsewhere.[9] With the assumption that an SPP wave propagates along the x axis with an $\exp(i\kappa x)$ variation and is independent of y, the solution of the canonical problem yields values of the wavenumber κ. We found that for the chosen constitutive parameters of both partnering materials, five p-polarized and four s-polarized SPP waves are allowed. Their relative wavenumbers κ/k_0 are provided in Table 1.

Table 1 Relative wavenumbers κ/k_0 at $\lambda_0 = 633$ nm of possible SPP waves guided by the planar interface of aluminum ($\epsilon_{\text{met}} = -56 + 21i$) and a rugate filter ($\Omega = \lambda_0$, $n_a = 1.45$ and $n_b = 2.32$) from the solution of the canonical boundary-value problem.[9]

***s*-pol**	$1.48639 + 0.00132i$	$1.7324 + 0.004i^*$	$1.9836 + 0.0006i^*$
	$2.2128 + 9.6 \times 10^{-5} i^*$		
***p*-pol**	$1.36479 + 0.00169i$	$1.61782 + 0.00548i$	$1.87437 + 0.00998i$
	$2.06995 + 0.01526i$	$2.21456 + 0.00246i$	

*These solutions had been missed when solutions for Fig. 1 of Ref. 9 were numerically searched.

3.2 *Grating-Coupled Configuration*

The compound surface-relief grating was chosen with $N_1 = N_2 = 3$, $\Lambda_1 = 0.75\lambda_0$, $\Lambda_2 = \lambda_0$, and $L_g = 50$ nm; furthermore, $d_3 - d_2 = 30$ nm. These specific parameters are consistent with experience acquired from working with simple surface-relief gratings.[10]

Plots of A_p and A_s as functions of θ are presented in Figs. 2 and 3, respectively, for $d_1 \in \{4\Omega, 6\Omega\}$. These plots contain several peaks. The peaks that are independent of the

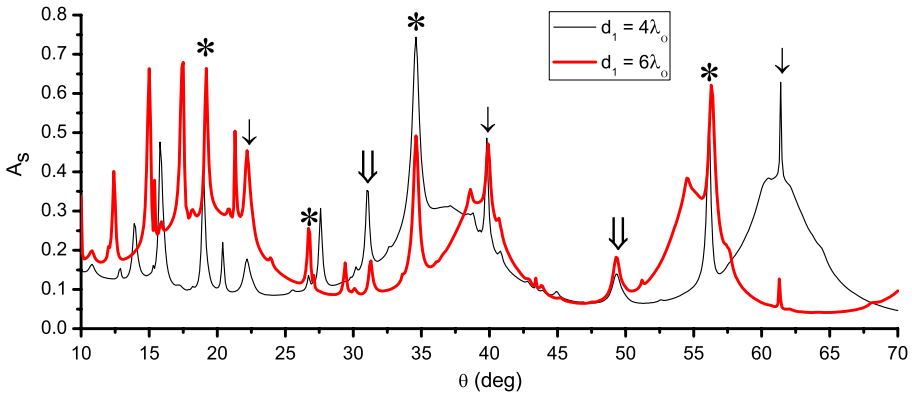

Fig. 2 A_s versus θ, when $N_1 = N_2 = 3$, $\Lambda_1 = 0.75\lambda_0$, $\Lambda_2 = \lambda_0$, $L_g = 50$ nm, $d_3 - d_2 = 30$ nm, and $\lambda_0 = 633$ nm. The vertical arrows and the stars identify the peaks that represent the excitation of *s*-polarized SPP waves: the arrows with single line (double line) represent the peaks that are also present in the absorptance curves when the compound grating is replaced with a simple grating with $N_2 = 0$ ($N_1 = 0$), but the stars represent the peaks that are not present when either $N_1 = 0$ or $N_2 = 0$.

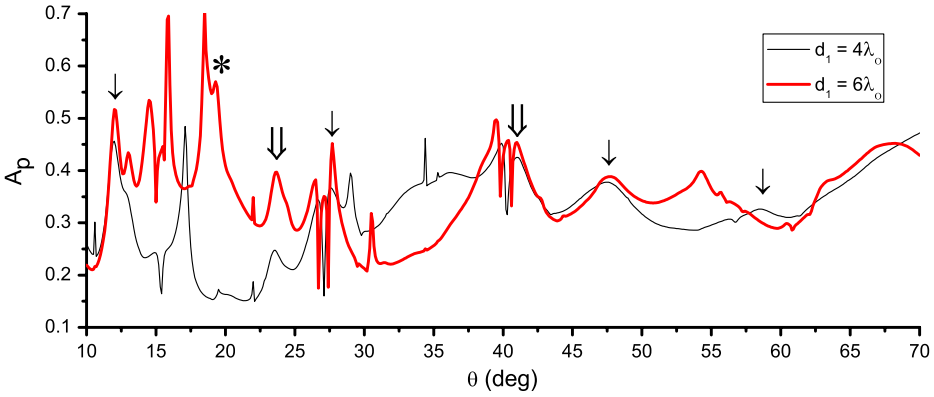

Fig. 3 Same as Fig. 2, except that A_p is plotted instead of A_s.

thickness of the partnering dielectric material beyond a certain threshold thickness indicate the excitation of SPP waves,[10] whereas the remaining peaks could represent the excitation of waveguide modes[25,26] that must depend on the thickness of the partnering dielectric material.

3.2.1 *Excitation of* s*-polarized SPP waves*

In the plots of A_s versus θ in Fig. 2, nine peaks, identified by vertical arrows and stars, are present independent of the thickness of the partnering dielectric material (i.e., the rugate filter). The angular positions of these A_s-peaks are $\theta = 19.0$ deg, 22.2 deg, 26.7 deg, 31.0 deg, 34.6 deg, 39.8 deg, 49.3 deg, 56.1 deg, and 61.4 deg; all angular positions in this paper were read from absorptance plots with the angle of incidence varying in steps of 0.1 deg. The conclusion that the identified peaks represent the excitation of *s*-polarized SPP waves is upheld by the spatial profiles of the *x*-component of the time-averaged Poynting vector in one unit cell ($0 < x < L$, $0 < z < d_3$).

In Fig. 4, the variation of $P_x(x,z) = \hat{\mathbf{u}}_x \dot{\mathbf{P}}(x,z)$ is provided for two values of θ: 19.0 deg and 22.2 deg. The figure confirms that the power density of the *s*-polarized SPP waves is maximal in the region near the plane $z = d_1$ and decays away from that region. Moreover, most of the energy of each SPP wave resides in the rugate filter rather than in the metal. As the spatial profiles in the top and bottom panels of Fig. 4 are different for the different values of θ, each of the two values of θ is associated with the excitation of different SPP waves.

In Fig. 5, the spatial variation of P_x is provided for two other values of θ: 39.8 deg and 56.1 deg. This figure again shows that an *s*-polarized SPP wave is excited at each of these two values of θ; however, the same *s*-polarized SPP wave is excited at both of these angles of incidence. This observation is not surprising as it has already been shown elsewhere[10] that the same SPP wave can be excited in the grating-coupled configuration at different angles of incidence.

Let us also note that $P_x > 0$ in all the spatial profiles presented in Figs. 4 and 5 implying that these SPP waves propagate parallel to $\hat{\mathbf{u}}_x$. This was found true for all *s*-polarized SPP waves excited at the peaks identified in Fig. 2 by vertical arrows and stars.

In the grating-coupled configuration, an SPP wave is excited whenever the real part of the wavenumber κ from the canonical boundary-value problem matches the wavenumber $k_x^{(n)}$ of the Floquet harmonic of order n for some $n \in [-N_t, N_t]$. These wavenumbers of the Floquet harmonics depend on the period L of the surface-relief grating. Also, if the SPP wave is propagating parallel to $\hat{\mathbf{u}}_x$ ($-\hat{\mathbf{u}}_x$) in our formulation of the problem, it is excited as a Floquet harmonic of positive (negative) order.

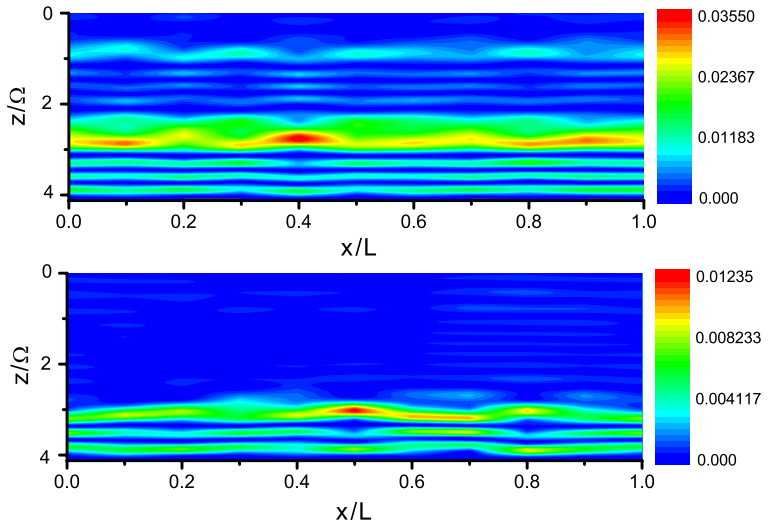

Fig. 4 Variation of the *x*-component P_x (in W m^{-2}) of the time-averaged Poynting vector $\mathbf{P}(x,z)$ when (top) $\theta = 19.0$ deg and (bottom) $\theta = 22.2$ deg, the incident plane wave is *s* polarized ($a_s^{(0)} = 1$ V m^{-1}, $a_p^{(0)} = 0$), and $d_1 = 4\Omega$. Other parameters are the same as for Fig. 2.

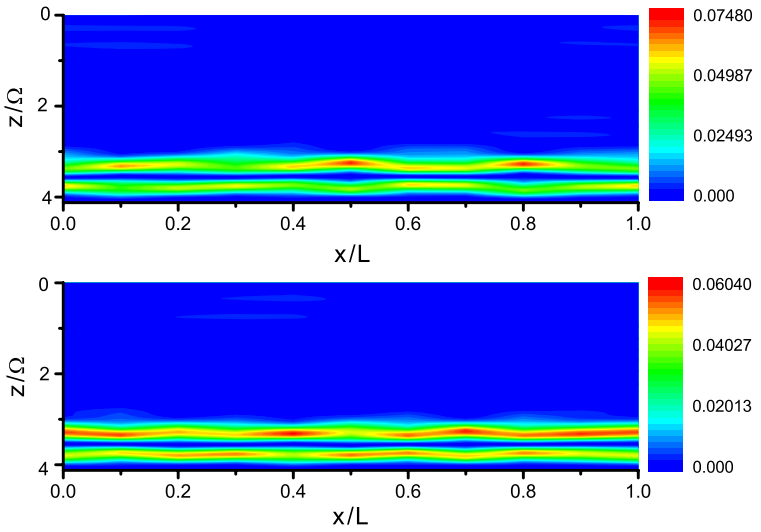

Fig. 5 Same as Fig. 4, except that (top) $\theta = 39.8$ deg and (bottom) $\theta = 56.1$ deg.

In the light of the foregoing discussion, let us now explain the roles of the two simple surface-relief gratings constituting the compound surface-relief grating in the excitation of multiple SPP waves. The relative wavenumbers $k_x^{(n)}/k_0$ of several Floquet harmonics are provided in Table 2 for:

- Case 1: $N_1 = 1$ and $N_2 = 0$ (i.e., $L = \Lambda_1$) and
- Case 2: $N_1 = 0$ and $N_2 = 1$ (i.e., $L = \Lambda_2$),

at the values of θ identified by vertical arrows and stars in Fig. 2. Plots of A_s versus θ for these two cases are provided in Fig. 6 to compare the A_s-peaks for the compound surface-relief grating with those for the individual simple surface-relief gratings. For the computation of absorptances when either $N_1 = 0$ or $N_2 = 0$, $N_t = 8$ was sufficient because the period L is much smaller than for the compound grating and a converged solution can be obtained with a smaller value of N_t. We also identify

- Case 3: $N_1 = N_2 = 3$,

which is the case of the chosen compound surface-relief grating, for ease of discussion. The relative wavenumbers of several Floquet harmonics are at the θ-positions of the A_s-peaks identified by stars are provided in Table 3 for case 3 only.

The solution of the canonical boundary-value problem predicts the existence of an s-polarized SPP wave with $\kappa/k_0 = 1.7324 + 0.0014i$. According to Table 2, the simple surface-relief grating of period Λ_1 alone is responsible for its excitation in the grating-coupled configuration at $\theta = 22.2$ deg in Fig. 2, because $k_x^{(1)}/k_0|_{\text{Case1}} = 1.7112$ is quite close to 1.7324. Furthermore, the leftmost A_s-peak identified in Fig. 6(a) by an arrow is at the same angular position as the A_s-peak of interest in Fig. 2.

Similarly, the solution of the canonical boundary-value problem predicts the existences of s-polarized SPP waves with $\kappa/k_0 = 1.9836 + 0.0006i$ and $2.2128 + 10^{-5}i$ (Table 1). A_s-peaks are present at $\theta = 39.8$ deg and 61.4 deg in Fig. 2. Both of these SPP waves are excited in the grating-coupled configuration due to the presence of the simple grating with period Λ_1 because $k_x^{(1)}/k_0|_{\text{Case1}} = 1.9734$ for $\theta = 39.8$ deg, and $k_x^{(1)}/k_0|_{\text{Case1}} = 2.2113$ for $\theta = 61.4$ deg in Table 2. Moreover, these A_s-peaks are also present at $\theta = 39.9$ deg and 61.4 deg in Fig. 6(a).

The two A_s-peaks identified by double arrows, at $\theta \in \{31.0 \text{ deg}, 49.3 \text{ deg}\}$, in Fig. 2 represent the excitation of s-polarized SPP waves due to the presence of simple grating of period Λ_2. A comparison of Tables 1 and 2 shows that $k_x^{(1)}/k_0|_{\text{Case2}} = 1.5150$ for $\theta = 31.0$ deg, and $k_x^{(1)}/k_0|_{\text{Case2}} = 1.7581$ for $\theta = 49.3$ deg are close to $\text{Re}(1.4864 + 0.0013i)$ and $\text{Re}(1.7324 + 0.0014i)$, respectively. These A_s-peaks identified by double arrows in Fig. 2 (at $\theta = 31.0$ deg and 49.3 deg) are also present in Fig. 6(b) at $\theta = 27.9$ deg and 45.5 deg,

Table 2 Relative wavenumbers $k_x^{(n)}/k_0$ of Floquet harmonics, at the θ-values of the peaks identified in Fig. 2 by vertical arrows and stars, when the compound surface-relief grating is replaced by just one of its two constituent simple surface-relief gratings. Case 1: $N_1 = 1$ and $N_2 = 1$. Case 2: $N_1 = 1$ and $N_2 = 1$. Boldface entries signify SPP waves.

	Case	$n = -2$	$n = -1$	$n = 0$	$n = 1$	$n = 2$
$\theta = 19.0$ deg	1	−2.3411	−1.0078	0.32557	1.6589	2.9922
	2	−1.6744	−0.67443	0.32557	1.3256	2.3256
$\theta = 22.2$ deg	1	−2.2888	−0.95549	0.37784	**1.7112**	3.0445
	2	−1.6222	−0.62216	0.37784	1.3778	2.3778
$\theta = 26.7$ deg	1	−2.2173	−0.88401	0.44932	1.7827	3.116
	2	−1.5507	−0.55068	0.44932	1.4493	2.4493
$\theta = 31.0$ deg	1	−2.1516	−0.8183	0.51504	1.8484	3.1817
	2	−1.485	−0.48496	0.5150	**1.5150**	2.5150
$\theta = 34.6$ deg	1	−2.0988	−0.76549	0.56784	1.9012	3.2345
	2	−1.4322	−0.43216	0.56784	1.5678	2.5678
$\theta = 39.8$ deg	1	−2.0266	−0.69322	0.64011	**1.9734**	3.3068
	2	−1.3599	−0.35989	0.64011	1.6401	2.6401
$\theta = 49.3$ deg	1	−1.9085	−0.5752	0.75813	2.0915	3.4248
	2	−1.2419	−0.24187	0.75813	**1.7581**	2.7581
$\theta = 56.1$ deg	1	−1.8367	−0.50332	0.83001	2.1633	3.4967
	2	−1.17	−0.16999	0.83001	1.8300	2.8300
$\theta = 61.4$ deg	1	−1.7887	−0.45535	0.87798	**2.2113**	3.5446
	2	−1.122	−0.12202	0.87798	1.878	2.878

respectively. The difference in the angular positions of each peak in the two figures is entirely due to the presence of the simple surface-relief grating of period Λ_1 in the compound surface-relief grating.

The A_s-peaks identified by stars in Fig. 2 at $\theta \in \{19.0 \text{ deg}, 26.7 \text{ deg}, 34.6 \text{ deg}, 56.1 \text{ deg}\}$ indicate the SPP waves that cannot be explained by either case 1 or case 2, because corresponding peaks are not present in Fig. 6(a) and 6(b). Instead, the entire compound surface-relief grating is involved as follows: At $\theta = 19.0$ deg, the SPP wave is excited as a Floquet harmonic of order $n = 6$ because $k_x^{(6)}/k_0|_{\text{Case3}} = 1.4684$ is close to $\text{Re}(1.4864 + 0.0013i)$ in Table 1; at $\theta = 26.7$ deg, the SPP wave is excited as a Floquet harmonic of order $n = 8$ because $k_x^{(8)}/k_0|_{\text{Case3}} = 1.9731$ is close to $\text{Re}(1.9836 + 0.0006i)$ in Table 1; at $\theta = 34.6$ deg, the SPP wave is excited as a Floquet harmonic of order $n = 6$ because $k_x^{(6)}/k_0|_{\text{Case3}} = 1.7107$ is close to $\text{Re}(1.7324 + 0.0014i)$ in Table 1; and at $\theta = 56.1$ deg, the SPP wave is excited as a Floquet harmonic of order $n = 6$ because $k_x^{(6)}/k_0|_{\text{Case3}} = 1.9729$ is close to $\text{Re}(1.9836 + 0.0006i)$ likewise. Thus, these SPP waves arise from a cooperative phenomenon which merges the distinct identities of the two constituent simple surface-relief gratings into a single identity. Let us also note that the excitation of the SPP wave at $\theta = 26.7$ deg is not as

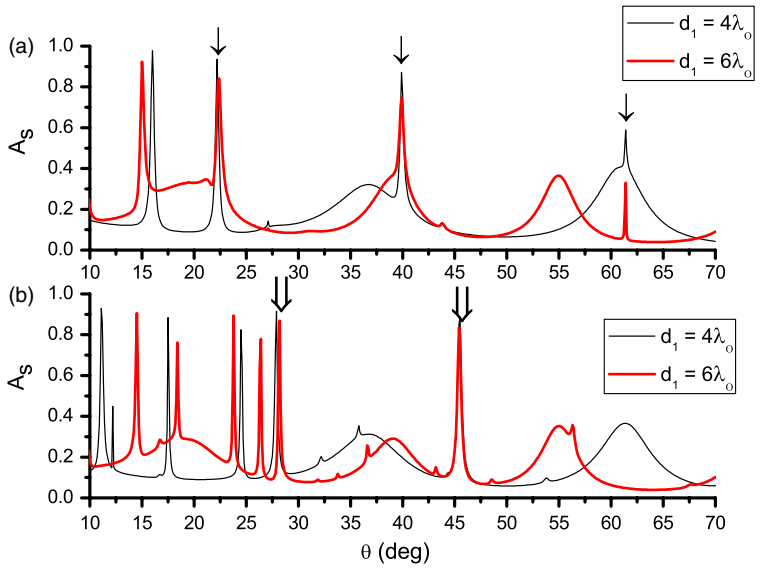

Fig. 6 A_s versus θ when $L_g = 50$ nm, $d_3 - d_2 = 30$ nm, $\lambda_0 = 633$ nm, for case 1 and case 2. The vertical arrows identify the peaks that represent the excitation of SPP waves.

Table 3 Relative wavenumbers $k_x^{(n)}/k_0$ of Floquet harmonics, at the θ-values of the peaks identified in Fig. 2 by stars when the s-polarized SPP waves are excited by the compound grating. Case 3: $N_1 = N_2 = 3$. Boldface entries signify SPP waves.

	Case	$n = 3$	$n = 4$	$n = 5$	$n = 6$	$n = 7$	$n = 8$
$\theta = 19.0$ deg	3	0.897	1.0875	1.2779	**1.4684**	1.6589	1.8494
$\theta = 26.7$ deg	3	1.0207	1.2112	1.4017	1.5922	1.7827	**1.9731**
$\theta = 34.6$ deg	3	1.1393	1.3297	1.5202	**1.7107**	1.9012	2.0917
$\theta = 56.1$ deg	3	1.4014	1.5919	1.7824	**1.9729**	2.1633	2.3538

Table 4 The relative wavenumbers κ/k_0 of *s*-polarized SPP waves in the canonical problem (Table 1) and the θ-values of the A_s-peaks in Figs. 6(a), 6(b), and 2 that represent the excitation of these SPP waves in cases 1, 2, and 3, respectively.

	θ		
κ/k_0	Fig. 6(a)	Fig. 6(b)	Fig. 2
$1.48639 + 0.00132i$	—	—	19.0 deg
	—	27.9 deg	31.0 deg
$1.7324 + 0.0014i$	22.2 deg	—	22.2 deg
	—	—	34.6 deg
	—	45.5 deg	49.3 deg
$1.9836 + 0.0006i$	—	—	26.7 deg
	39.9 deg	—	39.8 deg
	—	—	56.1 deg
$2.2128 + 9.6 \times 10^{-5} i$	61.4 deg	—	61.4 deg

efficient as at the other peaks identified by stars in Fig. 2 because the SPP wave is being excited as a Floquet harmonic of higher order when $\theta = 26.7$ deg than for the other three values of θ (Refs. 7, 10).

A comparison of the magnitudes of A_s at the absorptance peaks in Figs. 2 and 6 shows that an A_s-peak for an individual simple surface-relief grating (cases 1 and 2) is generally higher than the corresponding A_s-peak for the compound surface-relief grating (case 3).

In summary, nine A_s-peaks in Fig. 2 that represent the excitation of s-polarized SPP waves can be divided into three groups: (1) three peaks due to the presence of the simple surface-relief grating with period Λ_1, (2) two peaks due to the presence of the simple surface-relief grating with period Λ_2, and (3) four peaks due to the compound surface-relief grating itself with period $L = 3\Lambda_1 + 3\Lambda_2$. The relative wavenumbers κ/k_0 of s-polarized SPP waves in the canonical problem (Table 1) are correlated in Table 4 with the θ-values of the A_s-peaks in Fig. 2 that represent the excitation of these SPP waves in case 3. Correlation of some of those peaks with the A_s-peaks in Fig. 6(a) and 6(b), for cases 1 and 2, respectively, is also presented in the same table. All s-polarized SPP waves predicted by the solution of the canonical boundary-value problem can be excited by the compound surface-relief grating, but neither of the two constituent simple surface-relief gratings is, by itself, able to do the same. The A_s-peaks that are attributable to the simple surface-relief grating with period Λ_2 are shifted to somewhat higher angular positions, and the shift becomes more pronounced as the incidence becomes more oblique, whereas the peaks attributable to the other simple grating with period Λ_1 remain almost at the same angular position except for one peak that shifts to lower angular position.

3.2.2 *Excitation of* p*-polarized SPP waves*

In the plots of A_p versus θ provided in Fig. 3 for $d_1 \in \{4\Omega, 6\Omega\}$, the A_p-peaks that are independent of the thickness of the rugate filter are identified by vertical arrows and stars. Such A_p-peaks are present for $\theta \in \{12.0 \text{ deg}, 19.5 \text{ deg}, 23.5 \text{ deg}, 27.6 \text{ deg}, 41.0 \text{ deg}, 47,5 \text{ deg}, 56.3 \text{ deg}\}$ and represent the excitation of p-polarized SPP waves. Examination of the spatial profiles of $P_x(x,z)$ at these θ-values confirmed the localization of the power density to the plane $z = d_1$.

Representative profiles of P_x in a unit cell of the compound surface-relief grating are provided for two identified A_p-peaks in Fig. 7. The spatial profiles for $\theta = 23.5$ deg and $\theta = 27.5$ deg show that the power density of the p-polarized SPP wave is maximal in the region near the plane $z = d_1$ and decays away from that region. Moreover, P_x is predominantly positive implying that the p-polarized SPP waves are propagating along $\hat{\mathbf{u}}_x$ and are excited as Floquet

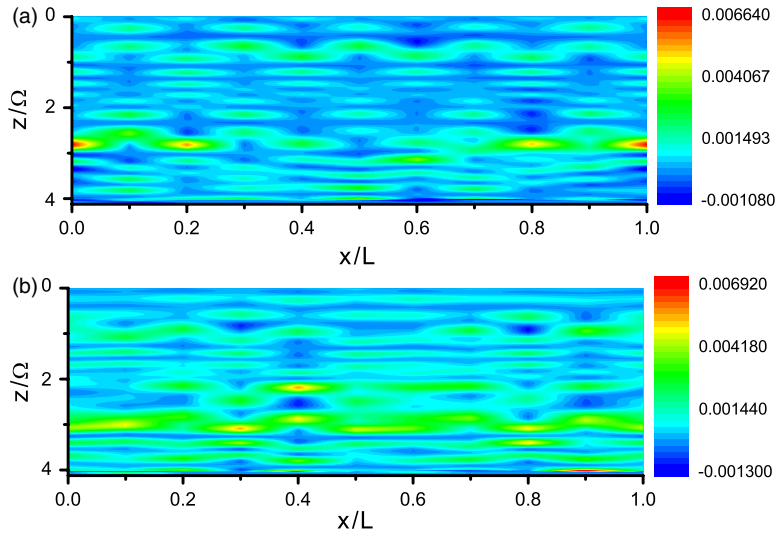

Fig. 7 Variation of the x-component P_x (in W m^{-2}) of the time-averaged Poynting vector $\mathbf{P}(x,z)$ when (a) $\theta = 23.5$ deg and (b) $\theta = 27.6$ deg, the incident plane wave is p polarized ($a_s^{(0)} = 0$, $a_p^{(0)} = 1$ V m^{-1}), and $d_1 = 4\Omega$. Other parameters are the same as for Fig. 3.

Table 5 Same as Table 2, except that the θ-values are of the A_p-peaks identified by vertical arrows and stars in Fig. 3.

	Case	$n=-2$	$n=-1$	$n=0$	$n=1$	$n=2$
$\theta = 12$ deg	1	−2.4588	−1.1254	0.20791	**1.5412**	2.8746
	2	−1.7921	−0.79209	0.20791	1.2079	2.2079
$\theta = 19.5$ deg	1	−2.3329	−0.99953	0.33381	1.6671	3.0005
	2	−1.6662	−0.66619	0.33381	1.3338	2.3338
$\theta = 23.5$ deg	1	−2.2679	−0.93458	0.39875	1.7321	3.0654
	2	−1.6013	−0.60125	0.39875	**1.3987**	2.3987
$\theta = 27.6$ deg	1	−2.2034	−0.87004	0.4633	**1.7966**	3.13
	2	−1.5367	−0.5367	0.4633	1.4633	2.4633
$\theta = 41.0$ deg	1	−2.0106	−0.67727	0.65606	1.9894	3.3227
	2	−1.3439	−0.34394	0.65606	**1.6561**	2.6561
$\theta = 47.5$ deg	1	−1.9294	−0.59606	0.73728	**2.0706**	3.4039
	2	−1.2627	−0.26272	0.73728	1.7373	2.7373
$\theta = 56.3$ deg	1	−1.8347	−0.50138	0.83195	**2.1653**	3.4986
	2	−1.168	−0.16805	0.83195	1.832	2.832

harmonics of positive order. This was found to be true for all other p-polarized SPP waves as well.

The relative wavenumbers $k_x^{(n)}/k_0$ of several Floquet harmonics are provided in Table 5 for case 1 and case 2 at the θ-values of the peaks identified in Fig. 3. Plots of A_p versus θ for these two cases are provided in Fig. 8 to compare the A_p-peaks for the compound surface-relief grating with those for the individual simple surface-relief gratings.

The A_p-peaks identified by single arrows in Fig. 3 are also present at approximately the same angular positions in Fig. 8(a). Therefore, the p-polarized SPP waves excited by the compound surface-relief grating for $\theta \in \{\text{red}\, 12.0 \text{ deg}, 27.6 \text{ deg}, 47.5 \text{ deg}, 56.3 \text{ deg}\}$ can be attributed solely to the simple surface-relief grating with period Λ_1. This is also evident from a comparison of Tables 1 and 5 because:

- $k_x^{(1)}/k_0|_{\text{Case1}} = 1.5412$ is close to $\text{Re}(1.61782 + 0.00548i)$ for $\theta = 12.0$ deg,
- $k_x^{(1)}/k_0|_{\text{Case1}} = 1.7966$ is close to $\text{Re}(1.87437 + 0.00998i)$ for $\theta = 27.6$ deg,
- $k_x^{(1)}/k_0|_{\text{Case1}} = 2.0706$ is close to $\text{Re}(2.06995 + 0.01526i)$ for $\theta = 47.5$ deg, and
- $k_x^{(1)}/k_0|_{\text{Case1}} = 2.1653$ is close to $\text{Re}(2.21456 + 0.00246i)$ for $\theta = 56.3$ deg.

A comparison of Figs. 3 and 8(b) shows that the A_p-peaks due to the independent simple surface-relief grating with period Λ_1 (case 1) are slightly shifted to lower angular positions when that simple grating becomes part of the compound surface-relief grating (case 3), the shift being larger at the higher angular locations.

Similarly, the A_p-peaks at $\theta = 23.5$ deg and 41.0 deg, identified by double arrows in Fig. 3, are also present at approximately the same angular positions in Fig. 8(b) signifying that the p-polarized SPP waves at these peaks are excited in effect by the presence of the simple surface-relief grating of period Λ_2. Moreover,

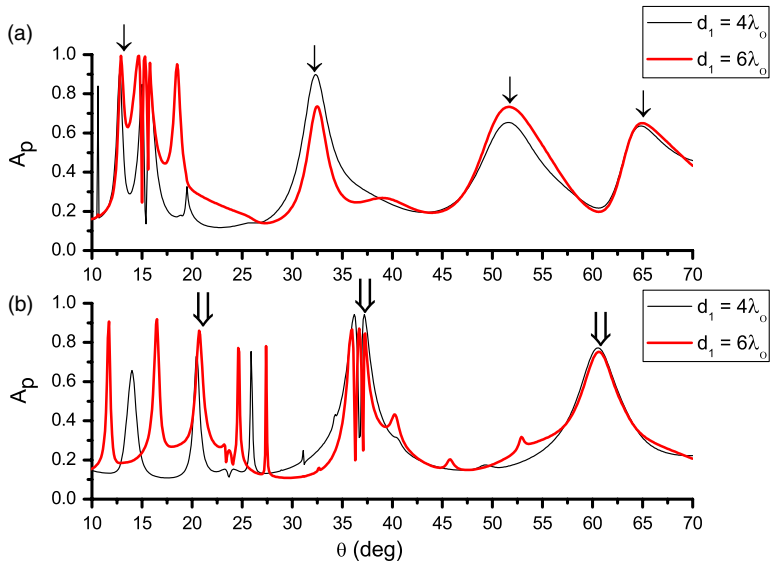

Fig. 8 Same as Fig. 6, except that A_p is plotted against θ.

- $k_x^{(1)}/k_0|_{\text{Case2}} = 1.3987$ is close to $\text{Re}(1.36479 + 0.00169i)$ for $\theta = 23.5$ deg, and
- $k_x^{(1)}/k_0|_{\text{Case2}} = 1.6561$ is close to $\text{Re}(1.61782 + 0.00548i)$ for $\theta = 41.0$ deg.

However, the A_p-peaks at $\theta = 20.5$ deg and $\theta = 37.2$ deg in Fig. 8(b) for the simple surface-relief grating with period Λ_2 shift to $\theta = 23.5$ deg and $\theta = 41.0$ deg, respectively, in Fig. 3 when this simple surface-relief grating becomes part of the compound surface-relief grating.

The A_p-peak identified by a star in Fig. 3 also represents the excitation of a p-polarized SPP waves; however, this peak is not present in the plots of A_p versus θ in Fig. 8 for either case 1 or case 2. Also, the A_p-peak at this value of θ is very low, suggesting that the SPP wave is being excited as a Floquet harmonic of a high order at this peak by the compound surface-relief grating with period $L = 3\Lambda_1 + 3\Lambda_2$. Indeed, the A_p-peak at $\theta = 19.5$ deg represents the excitation of a p-polarized SPP wave as a Floquet harmonic of order $n = 7$ by the compound grating because $k_x^{(7)}/k_0|_{\text{Case3}} = 1.6671$ is close to $\text{Re}(1.61782 + 0.00548i)$.

Table 6 The relative wavenumerbs κ/k_0 of p-polarized SPP waves in the canonical problem (Table 1) and the θ-values of the A_p-peaks in Figs. 8(a), 8(b), and 3 that represent the excitation of these SPP waves in cases 1, 2, and 3, respectively.

	θ		
κ/k_0	Fig. 8(a)	Fig. 8(b)	Fig. 3
$1.36479 + 0.00169i$	—	20.5 deg	23.5 deg
$1.61782 + 0.00548i$	12.8 deg	—	12.0
	—	—	19.5 deg
	—	37.2 deg	41.0 deg
$1.87437 + 0.00998i$	32.3 deg	—	27.6 deg
	—	60.6 deg*	—
$2.06995 + 0.01526i$	51.6 deg	—	47.5 deg
$2.21456 + 0.00246i$	64.8 deg	—	56.3 deg

*This A_p-peak in case 2 does not have a counterpart peak in case 3.

Let us note that an A_p-peak present in Fig. 8(b) at $\theta = 60.6$ deg for the simple surface-relief grating with period Λ_2 is not present in Fig. 3 for the compound surface-relief grating. Furthermore, as was shown for A_s-peaks in Sec. 3.2.1, an A_p-peak for an individual simple surface-relief grating (cases 1 and 2) is generally higher than the corresponding A_p-peak for the compound surface-relief grating (case 3). Thus, although the use of compound surface-relief gratings appears to be efficacious to excite SPP waves, careful selection of the constituent surface-relief gratings is needed for maximal effect.

To recapitulate, out of seven A_p-peaks in Fig. 3 that represent the excitation of p-polarized SPP waves, four peaks are due to the simple surface-relief grating with period Λ_1, two to the simple surface-relief grating period Λ_2 alone, and one to the compound surface-relief grating itself. The angular positions of the A_p-peaks representing the excitation of p-polarized SPP waves in Fig. 3 are presented in Table 6 are cross-referenced to values of κ/k_0 obtained from the solution of the canonical boundary-value problem. Correlation of some of those peaks with the A_p-peaks in Fig. 8(a) and 8(b), for cases 1 and 2, respectively, can also be deduced from the same table. A comparison of Tables 1 and 6 upholds the conclusions drawn in Sec. 3.2.1 for s-polarized SPP waves: All p-polarized SPP waves predicted by the solution of the canonical boundary-value problem can be excited by the compound surface-relief grating even though either of the individual surface-relief grating alone cannot excite all possible SPP waves. Furthermore, the A_p-peaks that are attributable to the simple surface-relief grating with period Λ_1 (Λ_2) shift to somewhat lower (higher) angular positions in Fig. 3 in relation to Fig. 8.

4 Concluding Remarks

The excitation of multiple SPP waves of the same frequency and the direction of propagation but of different linear polarization states, phase speeds, degrees of localization, and spatial profiles was studied theoretically in the grating-coupled configuration, when the surface-relief grating is compounded from two simpler surface-relief gratings and the partnering dielectric material is a rugate filter. The absorptances for s and p-polarized incident plane waves were calculated as functions of the angle of incidence for two sufficiently high values of the thickness of the partnering dielectric material to rule out waveguide modes and identify SPP waves.

Our numerical results allowed us to draw the following conclusions:

(1) With one fixed compound surface-relief grating, all the SPP waves predicted by the canonical boundary-value problem were excited. The extension of this conclusion to the compounding of two or more simple surface-relief gratings in different configurations requires further investigation.

(2) The excitation of each SPP wave could be attributed to either a simple surface-relief grating present in the compound surface-relief grating or to the compound surface-relief grating itself or to both.

(3) The same SPP wave could be excited by either one or both of the constituting simple gratings of the compound surface-relief grating and/or the compound grating itself.

(4) The angular positions of the absorptance peaks (signifying the excitation of SPP waves) for a simple surface-relief grating shifted somewhat when that grating was made a constituent of a compound surface-relief grating.

(5) Not every absorptance peak (indicative of the excitation of an SPP wave) for a simple surface-relief grating by itself had a counterpart peak for the compound surface-relief grating, but this conclusion does not nullify conclusion (1).

However, the excitation of any specific SPP wave turned out to be less efficient with the compound surface-relief grating than with a simple surface-relief grating. This observation is in agreement with the work of Dolev et al.[8] for whom the partnering dielectric material was homogeneous.

The foregoing conclusions are expected to be useful in enhancing the quantum efficiency of thin-film solar cells because of the greater possibility of exciting SPP waves of both linear polarization states. For this purpose, the rugate filter will have to be replaced by a multilayered semiconductor material and an easily manufacturable compound surface-relief grating will have to be

found to excite all possible SPP waves efficiently over a broad range of visible and infrared frequencies. The introduction of periodic nonhomogeneity in the partnering semiconductor would result in the possibility of guiding multiple SPP waves of both linear polarization states.[14] The possibility of exciting a given SPP wave by either a constituent simple surface-relief grating or the compound surface-relief grating at more than one angles of incidence (combined with the possibility of multiple SPP waves of the same frequency) will increase the energy coupled to SPP waves by the incident light not only in diffuse insolation but also in direct insolation when the solar cell is either unable or not designed to track the sun. The theoretical formulation of RCWA used in this paper for continuously nonhomogeneous partnering dielectric material has been recently extended for periodically multilayered dielectric materials.[27]

Acknowledgments

This work was partly supported by Grant No. DMR-1125591 from US National Science Foundation. A.L. is also grateful to Charles Godfrey Binder Endowment at the Pennsylvania State University for partial support of this work.

References

1. S. A. Maier, *Plasmonics: Fundamentals and Applications*, Springer, New York (2007).
2. J.Homola, *Surface Plasmon Resonance Based Sensors*, (Ed.), Springer, Heidelberg, Germany (2006).
3. P. Sheng, A. N. Bloch, and R. S. Stepleman, "Wavelength-selective absorption enhancement in thin-film solar cells," *Appl. Phys. Lett.* **43**(6), 579–581 (1983), http://dx.doi.org/10.1063/1.94432.
4. C. Heine and R. H. Morf, "Submicrometer gratings for solar energy applications," *Appl. Opt.* **34**(14), 2476–2482 (1995), http://dx.doi.org/10.1364/AO.34.002476.
5. S. Xiao, E. Stassen, and N. A. Mortensen, "Ultrathin silicon solar cells with enhanced photocurrents assisted by plasmonic nanostructures," *J. Nanophoton.* **6**(1), 061503 (2012), http://dx.doi.org/10.1117/1.JNP.6.061503.
6. M. A. Green and S. Pillai, "Harnessing plasmonics for solar cells," *Nature Photon.* **6**(3), 130–132 (2012), http://dx.doi.org/10.1038/nphoton.2012.30.
7. H. Raether, *Surface Plasmons on Smooth and Rough Surfaces and on Gratings*, Springer, Heidelberg, Germany (1988).
8. I. Dolev et al., "Multiple coupling of surface plasmons in quasiperiodic gratings," *Opt. Lett.* **36**(9), 1584–1586 (2011), http://dx.doi.org/10.1364/OL.36.001584.
9. M. Faryad and A. Lakhtakia, "On surface plasmon-polariton waves guided by the interface of a metal and a rugate filter with sinusoidal refractive-index profile," *J. Opt. Soc. Am. B* **27**(11), 2218–2223 (2010), http://dx.doi.org/10.1364/JOSAB.27.002218.
10. M. Faryad and A. Lakhtakia, "Grating-coupled excitation of multiple surface-plasmon-polariton waves," *Phys. Rev. A* **84**, 033852 (2011), http://dx.doi.org/10.1103/PhysRevA.84.033852.
11. J. A. Polo, Jr. and A. Lakhtakia, "Surface electromagnetic waves: a review," *Laser Photon. Rev.* **5**(2), 234–246 (2011), http://dx.doi.org/10.1002/lpor.v5.2.
12. A. Lakhtakia, "Surface multiplasmonics," *Proc. SPIE* **8104**, 810403 (2011), http://dx.doi.org/10.1117/12.893129.
13. T. G. Mackay and A. Lakhtakia, "Modeling chiral sculptured thin films as platforms for surface-plasmonic-polaritonic optical sensing," *IEEE Sensors J.* **12**(2), 273–280 (2012), http://dx.doi.org/10.1109/JSEN.2010.2067448.
14. M. Faryad and A. Lakhtakia, "Enhanced absorption of light due to multiple surface-plasmon-polariton waves," *Proc. SPIE* **8110**, 81100F (2011), http://dx.doi.org/10.1117/12.893492.
15. B. G. Bovard, "Rugate filter theory: an overview," *Appl. Opt.* **32**(28), 5427–5442 (1993), http://dx.doi.org/10.1364/AO.32.005427.
16. P. W. Baumeister, *Optical Coating Technology*, SPIE Press, Bellingham, WA (2004).

17. R. Overend et al., "Rugate filter fabrication using neutral cluster beam deposition," *Vacuum* **43**(1–2), 51–54 (1992), http://dx.doi.org/10.1016/0042-207X(92)90184-X.
18. E. Lorenzo et al., "Fabrication and optimization of rugate filters based on porous silicon," *Phys. Status Solidi C* **2**(9), 3227–3231 (2005), http://dx.doi.org/10.1002/(ISSN)1610-1642.
19. C.-C. Lee, C.-J. Tang, and J.-Y. Wu, "Rugate filter made with composite thin films by ion-beam sputtering," *Appl. Opt.* **45**(7), 1333–1337 (2006), http://dx.doi.org/10.1364/AO.45.001333.
20. M. G. Moharam and T. K. Gaylord, "Diffraction analysis of dielectric surface-relief gratings," *J. Opt. Soc. Am.* **72**(10), 1385–1392 (1982), http://dx.doi.org/10.1364/JOSA.72.001385.
21. L. Li, "Multilayer modal method for diffraction gratings of arbitrary profile, depth, and permittivity," *J. Opt. Soc. Am. A* **10**(12), 2581–2591 (1993), http://dx.doi.org/10.1364/JOSAA.10.002581.
22. M. G. Moharam, E. B. Grann, and D. A. Pommet, "Formulation for stable and efficient implementation of the rigorous coupled-wave analysis of binary gratings," *J. Opt. Soc. Am. A* **12**(5), 1068–1076 (1995), http://dx.doi.org/10.1364/JOSAA.12.001068.
23. F. Wang, M. W. Horn, and A. Lakhtakia, "Rigorous electromagnetic modeling of near-field phase-shifting contact lithography," *Microelectron. Eng.* **71**(1), 34–53 (2004), http://dx.doi.org/10.1016/j.mee.2003.09.003.
24. N. Chateau and J.-P. Hugonin, "Algorithm for the rigorous coupled-wave analysis of grating diffraction," *J. Opt. Soc. Am. A* **11**(4), 1321–1331 (1994), http://dx.doi.org/10.1364/JOSAA.11.001321.
25. N. S. Kapany and J. J. Burke, *Optical Waveguides*, Academic Press, New York, NY (1972).
26. D. Marcuse, *Theory of Dielectric Optical Waveguides*, Academic Press, San Diego, CA (1991).
27. M. Faryad et al., "Excitation of multiple surface-plasmon-polariton waves guided by the periodically corrugated interface of a metal and a periodic multilayered isotropic dielectric material," *J. Opt. Soc. Am. B* **29**(4), 704–713 (2012), http://dx.doi.org/10.1364/JOSAB.29.000704.

Muhammad Faryad received his BSc degree in mathematics and physics from University of Punjab, Pakistan, in 2002; MSc and MPhil degrees in electronics from Quaid-i-Azam University, Pakistan in 2006 and 2008, respectively; and PhD degree in engineering science and mechanics from the Pennsylvania State University, in 2012. He is a postdoctoral scholar at the Pennsylvania State University. His research experience includes analysis of high-frequency fields reflected from cylindrical reflectors in an isotropic chiral medium and the fractional curl operator in electromagnetics. Currently, his research interests are surface multiplasmonics, sculptured thin films, and thin-film solar cells.

Akhlesh Lakhtakia received degrees from the Banaras Hindu University (BTech and DSc) and the University of Utah (MS and PhD), in electronics engineering and electrical engineering, respectively. He is the Charles Godfrey Binder (Endowed) professor of Engineering Science and Mechanics at the Pennsylvania State University, and presently serves as the Editor-in-Chief of the *Journal of Nanophotonics*. His current research interests include nanotechnology, bioreplication, surface multiplasmonics, complex materials, metamaterials, and sculptured thin films. He is a Fellow of SPIE, Optical Society of America, Institute of Physics (UK), and American Association for the Advancement of Science.